# NOISE CHARACTERISTICS AND MEASUREMENT METHODOLOGY FOR TMR AND HALL-EFFECT CURRENT SENSORS

By Kevyn Robins
Allegro MicroSystems

## Introduction

Many electrical and power systems require accurate current sensing measurements, from electric vehicles to industrial automation. While both Hall-effect and tunnel magneto-resistance (TMR) current sensors provide excellent solutions for these measurements, their distinct noise characteristics must be carefully considered for optimal system performance.

Hall-effect sensors have been the industry standard for decades, offering reliable performance with relatively constant noise characteristics across frequency. However, TMR technology introduces new possibilities for high-precision measurements but with different noise behavior—most notably, a 1/f noise profile that dominates at low frequencies, compared to the white noise characteristics of Hall-effect sensors.

This application note provides a comprehensive guide for comparing noise characteristics between TMR and Hall-effect current sensors. It explains measurement techniques, analysis methods, and practical design considerations to help engineers make informed decisions when selecting current sensors for their specific applications.

## Understanding Noise Fundamentals

Noise in magnetic sensors originates from several fundamental sources. White noise is characterized by a constant power spectral density across all frequencies. Unlike frequency-dependent noise sources, the white noise spectral density $S_v(f)$ remains constant, resulting in a flat noise floor in frequency domain measurements:

$$S_v(f) = K$$

where K is a technology-dependent constant.

Another significant noise source, particularly relevant in TMR sensors, is 1/f noise (also called flicker noise). This noise component has a power spectral density that is inversely proportional to frequency:

$$S_v(f) = \frac{K}{f^{\alpha}}$$

where K is a technology-dependent constant, f is frequency, and $\alpha$ is typically close to 1.

The 1/f noise dominates at low frequencies and rolls off as frequency increases, eventually becoming less significant than the white noise floor.

The corner frequency is the frequency at which the white noise equals the flicker noise.

When specifying noise performance, two primary metrics are commonly used. Noise amplitude spectral density ($S_V(f)$) is expressed in V/√Hz or T/√Hz and represents the noise per unit bandwidth. The integrated noise, obtained by integrating the noise power spectral density over the measurement bandwidth, provides a complete picture of the sensor's noise performance in the application:

$$V_{\text{noise(RMS)}} = \sqrt{\int_{f_L}^{f_H} S_v(f)^2 df}$$

where $f_L$ and $f_H$ define the measurement bandwidth of interest.

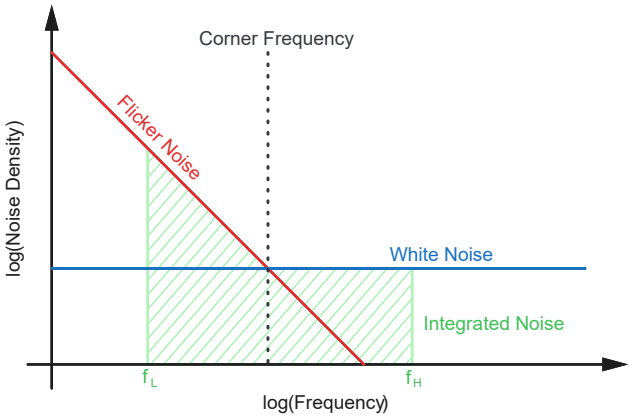


*Figure 1: Noise density of flicker noise and white noise*

## Noise Measurement Methodology

Accurate noise characterization requires careful consideration of measurement setup, equipment selection, and data acquisition parameters. The methodology presented here focuses on obtaining high-quality noise measurements across a wide frequency range, using only an oscilloscope.

The measurement system consists of a device under test (TMR or Hall-effect sensor), a low-noise power supply using LiPo battery and LDO regulators for minimal noise contribution, and a high-resolution digital oscilloscope for data acquisition. To minimize external noise sources and ensure measurement accuracy, the LiPo battery followed by low-dropout (LDO) regulators provides inherently low noise compared to switched-mode power supplies and eliminates power line interference.

The data acquisition uses a total of 20 million samples acquired over 100 seconds, resulting in a 200 kHz sampling rate. According to the Nyquist theorem, this allows spectral analysis up to 100 kHz. The long acquisition time combined with high sample count provides excellent frequency resolution at low frequencies while enabling sufficient averaging at high frequencies.

The noise spectral density is computed using a variant of Welch's method of averaging modified periodograms. The Welch's technique consists in dividing the time series into overlapping segments, applying a window function to each segment to reduce spectral leakage, computing the discrete Fourier transform (DFT) of each windowed segment, and averaging their squared magnitudes [1]. The averaging process reduces the variance of the spectral estimate at the expense of frequency resolution. The variant used here was developed to provide optimal frequency resolution for each Fourier frequency and more averaging at higher frequencies where the noise is typically flatter [2].

To establish measurement system limitations and validate the setup, noise measurements were performed in three configurations: with shorted inputs of the oscilloscope to determine the system noise floor, on the power supply output voltage to verify the low-noise power source, and finally on the sensor output voltage for actual device characterization.

The measurement system capability was validated by characterizing three distinct noise spectral densities, as shown in Figure 2. The oscilloscope's intrinsic noise floor was established by measuring its shorted inputs, providing a baseline reference (blue trace). The power supply noise, measured at VCC, demonstrates noise levels at or below the measurement system floor, confirming the effectiveness of the LiPo battery and LDO regulator configuration. Finally, the sensor output (VOUT) measurement clearly shows the noise characteristics of the CT427-30MR above the system noise floor, validating the measurement methodology. This simple yet effective setup enables accurate noise characterization across the frequency range of interest.

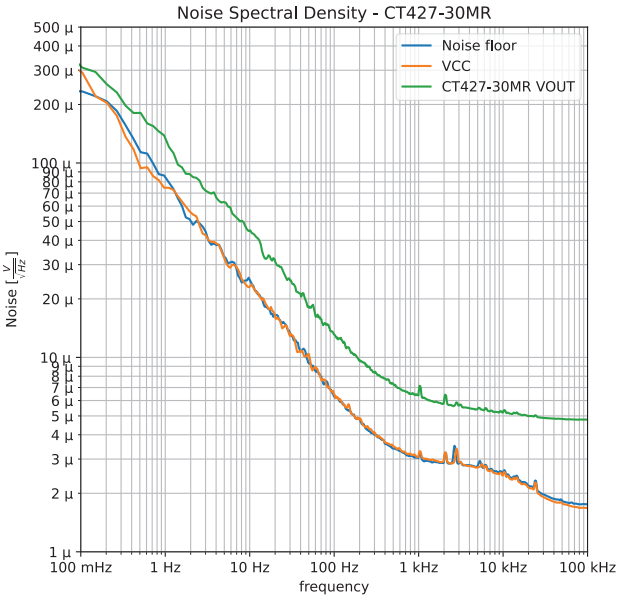


*Figure 2: Noise spectral densities of the measurement setup, the power supply, and the CT427 output*

## Magnetic Sensor Noise Characteristics and Technology Comparison

The noise performance of magnetic current sensors can be best understood through direct comparison of TMR and Hall-effect technologies. Figure 3 presents the noise spectral density measurements of four representative devices: three TMR sensors (CT4022-A10BSN8, CT433-HSWF20DR, and CT427-HSN830MR) and one Hall-effect sensor (ACS37010-30B5). All measurements are expressed in A/√Hz to enable direct comparison despite having different sensitivities. The current noise density is calculated by dividing the measured voltage noise density by each sensor's sensitivity.

$$S_i(f) = \frac{S_v(f)}{\text{Sensitivity}}$$

where:

- $S_I(f)$ is the current noise density in A/√Hz
- $S_V(f)$ is the measured voltage noise density in V/√Hz
- Sensitivity is the sensor transfer function in V/A

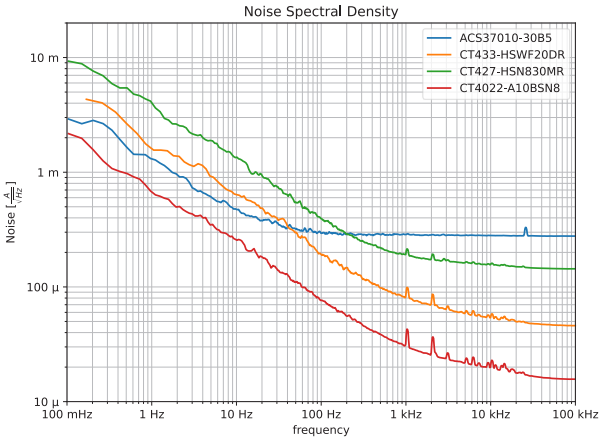


*Figure 3: Noise spectral densities of different Allegro current sensors*

TMR sensors exhibit characteristic 1/f noise behavior at low frequencies, transitioning to white noise at higher frequencies. The transition point, or corner frequency, varies among TMR devices due to differences in their magnetic stack design and signal conditioning circuitry.

In contrast, the Hall-effect sensor demonstrates predominantly white noise behavior across the frequency spectrum, offering consistent noise performance independent of frequency. A slight increase in noise density is observed below 30 Hz. This low-frequency behavior should not be interpreted as inherent to Hall-effect technology. Rather, it may originate from the internal signal conditioning circuitry, such as operational amplifiers and bias circuits, or from the measurement system itself.

The total integrated noise from 0.1 Hz to 100 kHz provides a comprehensive metric for comparing sensor performance in typical applications, by summing the contribution of each frequency to the total noise. Table 1 summarizes the measured RMS noise for each sensor:

***Table 1: Comparison of integrated noise of different Allegro current sensors***

| Sensor Model | Technology | Integrated Noise (mArms) | Integrated Noise (mVrms) |
|---|---|---|---|
| CT4022-A10BSN8 | TMR | 5.88 | |
| CT433-HSWF20DR | TMR | 16.54 | |
| CT427-HSN830MR | TMR | 47.74 | |
| ACS37010-30B5 | Hall | 87.67 | |

These measurements demonstrate the superior noise performance of TMR technology, with the CT4022-A10BSN8 achieving nearly 15 times lower integrated noise compared to the Hall-effect sensor. The variation among TMR sensors reflects different design optimizations for specific application requirements, balancing factors such as bandwidth, sensitivity, and dynamic range. While the Hall-effect sensor shows higher integrated noise, its other specifications continue to make it an excellent choice for applications where ultimate resolution is not the primary consideration.

The noise characteristics observed in the frequency domain are reflected in the time domain waveforms shown in Figure 4. The Hall-effect sensor (ACS37010-30B5) exhibits a relatively uniform noise distribution characteristic of white noise, with peak-to-peak variations of approximately 40 mV. The CT4022-A10BSN8 demonstrates the lowest peak-to-peak noise variation among all sensors, consistent with its superior integrated noise performance. These time domain measurements provide an intuitive visualization of the noise behavior and complement the spectral analysis in assessing sensor performance for specific applications.

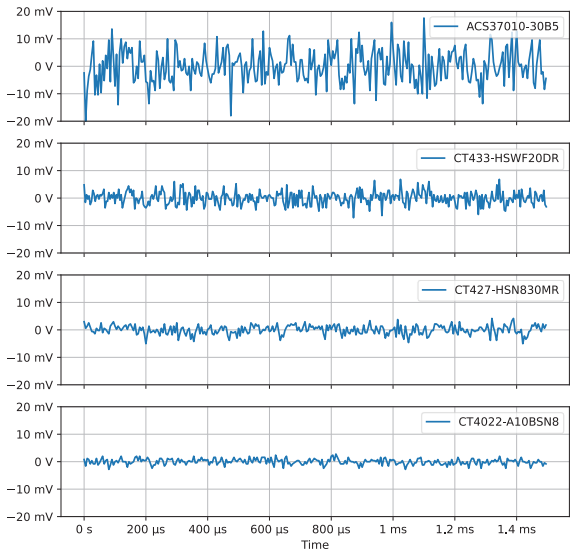


*Figure 4: Noise waveforms in the time domain for different Allegro current sensors*

## Conclusion

This analysis demonstrates distinct noise characteristics between TMR and Hall-effect current sensor technologies. The rigorous measurement methodology used shows that TMR sensors like the CT4022-A10BSN8 achieve up to 15 times lower integrated noise levels compared to traditional Hall-effect sensors, despite exhibiting characteristic 1/f noise at low frequencies. While Hall-effect sensors display more consistent noise across frequency ranges, the choice between technologies ultimately depends on specific application requirements. This comparative analysis provides engineers with quantitative data to make informed decisions for their current sensing applications.

## Bibliography

[1] P. Welch, The use of fast Fourier transform for the estimation of power spectra: A method based on time averaging over short, modified periodograms, IEEE Transactions on Audio and Electroacoustics, vol. 15, no. 2, pp. 70-73, June 1967, doi: 10.1109/TAU.1967.1161901.

[2] Michael Tröbs, Gerhard Heinzel, Improved spectrum estimation from digitized time series on a logarithmic frequency axis, Measurement, Volume 39, Issue 2, 2006, Pages 120-129, ISSN 0263-2241, doi: 10.1016/j.measurement.2005.10.010.

*Revision History*

| Number | Date | Description |
|---|---|---|
| – | July 23, 2025 | Initial release |



955 PERIMETER ROAD • MANCHESTER, NH 03103 • USA
+1-603-626-2300 • FAX: +1-603-641-5336 • ALLEGROMICRO.COM